

Review

Exploring the Potential of 3D Printing Technology for Sustainable Plastic Roads: A Preliminary Investigation

Mohamed Ezzat Al-Atroush ^{1,2,*} , Jumana Almushcab ³, Duha Alhudaif ⁴ and Yosra Meskinyar ⁴

¹ Civil and Environmental Engineering Program, College of Engineering, Prince Sultan University, Riyadh 11543, Saudi Arabia

² Department of Engineering Management, College of Engineering, Prince Sultan University, P.O. Box 66833, Riyadh 12211, Saudi Arabia

³ Software Engineering, College of Computer and Information Systems, Prince Sultan University, Riyadh 11543, Saudi Arabia

⁴ Architectural Engineering Department, College of Architecture and Design, Prince Sultan University, Riyadh 11543, Saudi Arabia

* Correspondence: mezzat@psu.edu.sa

Abstract: The urgency of climate change has highlighted the need for sustainable road construction materials, replacing the conventional asphalt, which significantly contributes to global warming and the urban heat island effect. With this in mind, the construction of the world's first 30-m plastic road in Zwolle, Netherlands, in 2018, opened the door for novel plastic applications as paving materials. However, its application is currently still limited to sidewalks and light-load cycling lanes. The feasibility of utilizing 3D printing technology to provide the necessary structural design flexibility for the production of plastic pavement modules that can withstand heavy traffic and extreme weather conditions was examined in this preliminary study. The suitability of six plastic materials (PLA, PETG, ABS, TPU, Nylon, and polycarbonate) for 3D printing was evaluated. Polylactic acid (PLA), and polyethylene terephthalate glycol (PETG) were identified as the most suitable materials for this study. Three small-scale structural systems, namely hollow modular with plastic columns, hollow modular with solid plastic cones, and hollow modular with X-bracing, were designed and successfully printed using the adopted materials and a 3D printer. The developed systems were subsequently subjected to compression testing to assess their structural performance under heavy traffic loads and demonstrate the feasibility of the concept. The results showed that the PLA conic structural system was effective and exhibited the highest compression strength, while the PETG conic system exhibited ductile behavior with superior thermal stability. The study suggests that the hybrid system of PLA and PETG materials may improve the overall performance, combine flexibility and strength, and potentially improve the resistance to extreme weather and heavy traffic. These findings prove that 3D printing technology has the potential to revolutionize the road construction industry and provide more sustainable solutions for infrastructure development.

Keywords: 3D printing technology; plastic roads; sustainable pavement systems; future cities



Citation: Al-Atroush, M.E.; Almushcab, J.; Alhudaif, D.; Meskinyar, Y. Exploring the Potential of 3D Printing Technology for Sustainable Plastic Roads: A Preliminary Investigation. *Sustainability* **2023**, *15*, 16777. <https://doi.org/10.3390/su152416777>

Academic Editors: Marc A. Rosen, Amos Darko, Sayanthan Ramakrishnan, K. Venkatachalam, Baojie He and Siliang Yang

Received: 24 September 2023

Revised: 18 November 2023

Accepted: 11 December 2023

Published: 13 December 2023



Copyright: © 2023 by the authors. Licensee MDPI, Basel, Switzerland. This article is an open access article distributed under the terms and conditions of the Creative Commons Attribution (CC BY) license (<https://creativecommons.org/licenses/by/4.0/>).

1. Introduction

Asphalt is a commonly used construction material for roads because of its durability, cost-effectiveness, and well-defined construction method. However, the production and construction of asphalt also contribute to climate change. The manufacturing process of asphalt involves heating petroleum, a fossil fuel that releases greenhouse gases such as carbon dioxide and sulfur dioxide into the atmosphere [1]. Moreover, asphalt roads absorb and retain heat, leading to the urban heat island effect [2,3], which can negatively impact human health and increase energy consumption for cooling.

The production and construction of asphalt are associated with significant environmental impacts, particularly greenhouse gas emissions. These emissions are generated

throughout the lifecycle of asphalt construction, with the mixing phase being the most significant contributor to emissions, accounting for approximately 95.04% of the total emissions. The transportation phase also contributes to emissions, accounting for 2.38% of the total [4]. Studies have shown that the carbon footprint of hot mix asphalt (HMA) layer construction is approximately 65.8 kg of CO₂ per kilometer of road [1–5]. These emissions are a major contributor to global warming, leading to the trapping of heat in the Earth's atmosphere and contributing to the impacts of climate change.

Asphalt pavements, on the other hand, are also sensitive to temperature changes. They are expected to fail earlier as a result of climate change [6]. The increase in greenhouse gas (GHG) emissions has led to rising global temperatures, affecting the structural performance of asphalt itself. A recent evaluation study conducted by Transportation for America [7] to assess the status of American roads between 2009 and 2017 found that the percentage of roads in poor condition increased from 14 to 20 percent. The inappropriate selection of paving materials, typically prescribed under the assumption of a stationary climate rather than considering the potential effects of climate change, was reported as the main reason for this increase. Considering the temperature sensitivity of the flexible pavement, several failures and distresses could be predicted [8–10]. Gudipudi et al., 2017 [11] have demonstrated that the anticipated rise in temperature during summertime heatwaves could significantly shorten the pavement life from 16 to 4 years and raise the maintenance costs by 100%.

In the same line, conventional asphalt pavement has an impermeable surface. As a result, if proper drainage measures are not implemented, water can accumulate on the pavement's surface and create hazardous driving conditions. Furthermore, standing water on asphalt pavements can accelerate pavement deterioration and reduce the lifespan of the pavement. With this in mind, in recent years, major flooding events have been witnessed in various geographical regions, such as Hurricanes Harvey (Texas), Irma (Florida), Katrina (Louisiana), and Sandy (New England); these events caused extensive social and economic damages, resulting in billions of dollars in infrastructure losses [12].

As climate change becomes an increasingly urgent global issue, there is a need for alternative road construction materials that are more environmentally friendly and sustainable and able to withstand extreme weather conditions. One such alternative is prefabricated plastic pavement, which is made entirely of plastic materials, either virgin or recycled plastics. The world's first 30-m plastic road was constructed and launched in Zwolle, Netherlands, in September 2018 [13]. KWS2, Wavin, and Total worked together on the PlasticRoad project, which was conceptualized by KWS2's Simon Orritsma and Anne Koudstaal. These prefabricated plastic panels have been found to be lighter, last longer, and have better water drainage capabilities than traditional asphalt surfaces [9,14]. In the presence of the global plastic waste problem and the 300 billion tons annually produced, the use of plastic roads can also help to address the growing problem of plastic waste by finding a new use for recycled plastic materials.

This successful real-world example demonstrates the potential of plastic roads to provide a sustainable solution for road construction that addresses the problem of plastic waste. However, the use of plastic roads is still a relatively new technology, limited to light-load walkways and cycle paths. More research is needed to fully understand plastic roads' potential benefits and drawbacks and how to extend this new technology to heavy-traffic roadways. These plastic roads are expected to have a longer lifespan than traditional asphalt roads, but evaluating their performance under extreme weather and heavy traffic conditions and their long-term environmental impact is still essential.

This paper investigates the feasibility of utilizing 3D printing technology in manufacturing plastic roadway panels able to withstand extreme weather conditions and heavy traffic loads. The study introduces a sustainable and eco-friendly approach to road construction, incorporating a hollow modular road structure from plastic waste. This plastic road has superior water storage capacity to mitigate flooding and is equipped with data collection and maintenance scheduling sensors, making it an ideal fit for smart and future

cities. The study also explores various plastic materials and structural systems to achieve the optimum design for heavy traffic and extreme weather conditions. Ultimately, the successful utilization of this system could lead to a global reduction in plastic waste and greenhouse gas emissions while improving infrastructure sustainably and cost-effectively.

2. Literature Review

Prefabricated plastic pavement is a modular and hollow road structure that is constructed from either virgin or recycled plastic materials. Unlike traditional pavement structures, it is designed to be modular and lightweight. Plastic pavement's prefabrication production and modular design make it more efficient, faster to construct, and simpler to maintain [15]. Prefabricated plastic pavement typically consists of hollow spaces directly underneath the top surface of the subgrade. These hollow spaces can be utilized for various purposes, such as the passage of cables and pipes, which prevents damage caused by digging, and the storage of water to prevent the risk of flooding. The details of the prefabricated panel are given in Figure 1.

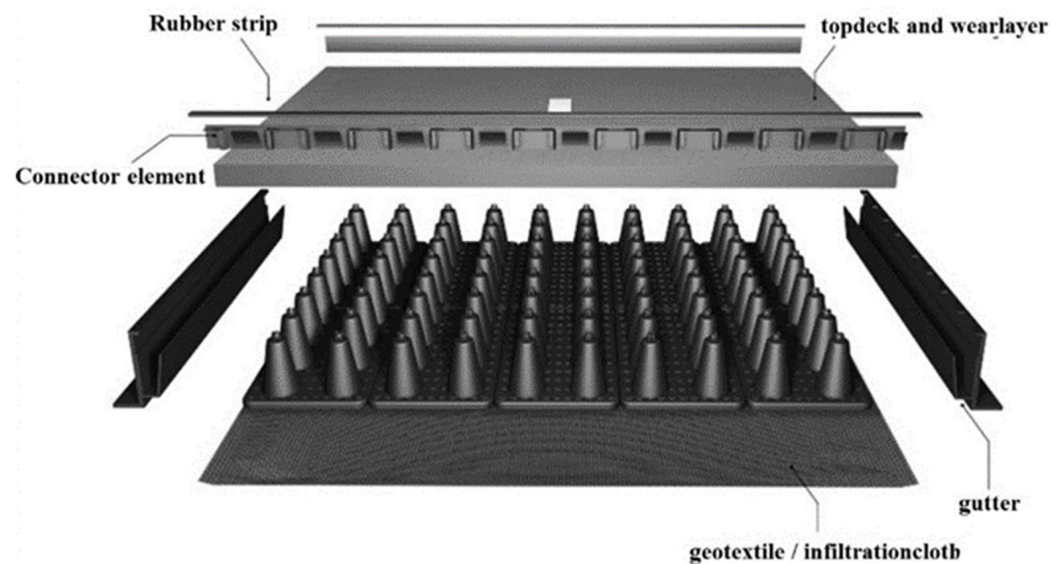


Figure 1. The currently available design of the prefabricated plastic panel for the cycle path (after [14]).

Once the prefabricated panels are manufactured, they are transported to the construction site and assembled in the anticipated pattern. The plastic panels are interlocked to create a seamless, durable, sustainable surface. Since the panels are modular in design, they can be easily replaced or repaired if necessary, as shown in Figure 2. The assembled panels are then placed on top of a geotextile or geomembrane layer, which functions as a water barrier layer.

The construction method for plastic roads involves a modular and hollow road structure that is prefabricated in a factory setting, resulting in a faster and more efficient construction process compared to traditional pavement methods. The first step in the construction process is the collection and processing of plastic waste. This waste is usually sourced from various materials, such as plastic bottles, old fishing nets, and other plastic products. The prefabrication process involves the use of a specialized machine that shreds and melts the plastic waste, which is then molded into the desired shape of the road panels. The panels are then cooled and cut to the required length [14]. The second step in the construction process is the preparation of the subgrade or the soil and foundation beneath the road surface. The subgrade must be compacted and leveled to ensure a stable base for the plastic road. Next, a geotextile is placed on top of the subgrade to separate the subgrade and the road surface. This helps to prevent soil erosion and water infiltration and allows for a better contact stress distribution on the bottom panel base [14]. The final step in the construction process is filling the hollow spaces within the plastic panels. These spaces can be used for

various purposes, such as the passage of cables and pipes, and also serve as a storage vessel for water, which helps to prevent flooding.



Figure 2. The currently available construction method of the prefabricated plastic panel for the cycle path (after [14]).

According to [14], CCL100, CCL200, and CCL300 are the three available types of panels typically designed and manufactured for such systems. CCL100 is a model of PlasticRoad's modular infrastructure solution. It is a lightweight panel made of recycled plastic that is designed for use as a bike or pedestrian path. The hollow space inside the panel can be used to store rainwater during heavy rain showers, preventing flooding temporarily. The panel's low weight enables it to be applied on soft soils without additional foundation measures. Usually, this model is used as a transition element between the main plastic path and the asphalted path.

CCL200 (Figure 3a) is a sustainable alternative to traditional road paving that is designed to be used in conjunction with an existing rainwater sewer system. It facilitates the collection of rainwater and allows for partial infiltration into the local subsurface. On the other hand, CCL300 is a premium product that is specifically engineered for climate adaptation. It features an integrated water filtration system that captures, purifies, and gradually infiltrates water into the local subsurface. It is also equipped with smart sensors that enhance the management and maintenance of the road surface. CCL300 also has the capability to collect rainwater and facilitate infiltration into the local subsurface (see Figure 3b). Table 1 compares the three alternatives of prefabricated plastic panels [14].



Figure 3. Alternatives of prefabricated plastic panels. (a) CCL200. (b) CCL300.

Plastic road technology is still in the very early stage. However, there are a few real-life cases that have been successfully demonstrated. This section discusses the lessons learned from ten real-life cases aiming for the further improvement of this promising approach. Table 2 summarizes the key facts of the ten case studies constructed using plastic road technology in different locations.

Table 1. A comparison between the three variants, CCL100, CCL200, and CCL 300 (after [14]).

| Feature | CCL100 | CCL200 | CCL300 |
|----------------------------|--------------|----------------------------------|---------------|
| Climate Adaptation | Low | Moderate | High |
| Rainwater Drainage | Not included | Additional to the existing sewer | Integrated |
| Water Filter System | Not included | Not included | Included |
| SMART Sensors | Not included | Not included | Included |
| Infiltration Functionality | Not included | Partially | Guaranteed |
| Overflow to Existing Sewer | Necessary | Necessary | Not necessary |
| Flexibility | Moderate | Moderate | High |

Table 2. A summary of ten case studies of plastic roads (after [14]).

| # | Case Study | Application | Location | Model Type | Size (m/m ²) | Water Storage (Liter) |
|------|--|--|--------------------------------|------------|----------------------------------|-------------------------|
| 1 | The municipality of Vlissingen | Combination bike and footpath | Ritthem, Netherlands | CCL100 | 200 sqm | N/A |
| 2 | The Antwerp Port Authority invests in safe cycle paths | Bike path | Antwerp, Belgium | CCL300 | 75 m | 64,600 |
| 3 | New lightweight bike path in the green area of Gouda | Bike path | Gouda, Netherlands | CCL300 | 100 m | 91,000 |
| 4 | Combination of bicycle and pedestrian path in Zeeland | Combination of cycle path and footpath | Ritthem, Netherlands | CCL00 | 200 sqm | NA |
| 5 | Climate-adaptive parking bays in Rotterdam | Longitudinal parking | Jan van Vuchtstraat, Rotterdam | CCL300 | 10 parking bays Water storage | 27,000 |
| 6 | Intelligent cycle path on the TU Delft campus | Bicycle path | Delft | CCL300 | 25 m | 12,942 |
| 7 | Sustainable carpool place in Hardenberg | 8 parking bays | Hardenberg | CCL300 | 27,240 sqm | NA |
| 8 | Parking spaces at VolkerWessels Infra campus, Vianen | Bike path (pilot) | Vianen | CCL300 | NA | Temporarily storage |
| 9 | Mexico City (pilot) Homeproject bike path, Mexico City (pilot) | Bike path | Giethoorn, Netherlands | CCL300 | NA | A solution for flooding |
| 10 * | Cycle path, Giethoorn (pilot) | Cycle path | Giethoorn, Netherlands | CCL300 | 30m | NA |

* Recycled waste: 1000 kg, CO₂ emission reduction: 72%. In addition, an extensive sensor network in the hollow space of the road elements was used for settlement monitoring.

The implementation of PlasticRoad technology in ten case studies has shown that it is a versatile solution that can be used in various infrastructure projects and effectively addresses climate change challenges. Different types of PlasticRoad elements are suited for different projects, and their ability to store and filter rainwater can prevent flooding and mitigate drought, as shown in Case No. 3, where only 100 m length was enough to store around 91,000 L of water [14]. The use of recycled plastic in the technology reduces CO₂ emissions and makes it sustainable. The use of sensors for data collection and analysis can lead to smarter and more efficient infrastructure maintenance and highlight the potential for PlasticRoad in smart cities. Overall, the case studies provide evidence of PlasticRoad's potential as a viable solution for infrastructure needs. However, all these cases were limited to sidewalk and bike lane applications in cold climate locations. This study aims to extend this new technology to fit the needs of extreme weather and heavy traffic applications.

3. Methodology

In contrast to the methods described in CCL100 to 300, which primarily focus on prefabricated approaches and recycled plastics, our study explores the innovative realm of 3D printing technology, employing two distinct types of plastic filament, namely polylactic acid (PLA) and polyethylene terephthalate glycol (PETG). While the previous literature

has emphasized prefabrication techniques and recycled plastics, our research focuses on applying advanced manufacturing processes and a wider array of materials. In addition, the specific structural designs introduced in our study, including conic elements, respond to the need for sustainability and enhanced structural performance in the context of heavy traffic and extreme weather conditions.

This study investigates the feasibility of utilizing 3D printing technology in manufacturing plastic road modules that can provide the structural design flexibility needed for the manufacturing of plastic modules with high thermal and structural stability. The methodology of this study was composed of three main phases, as demonstrated in Figure 4.

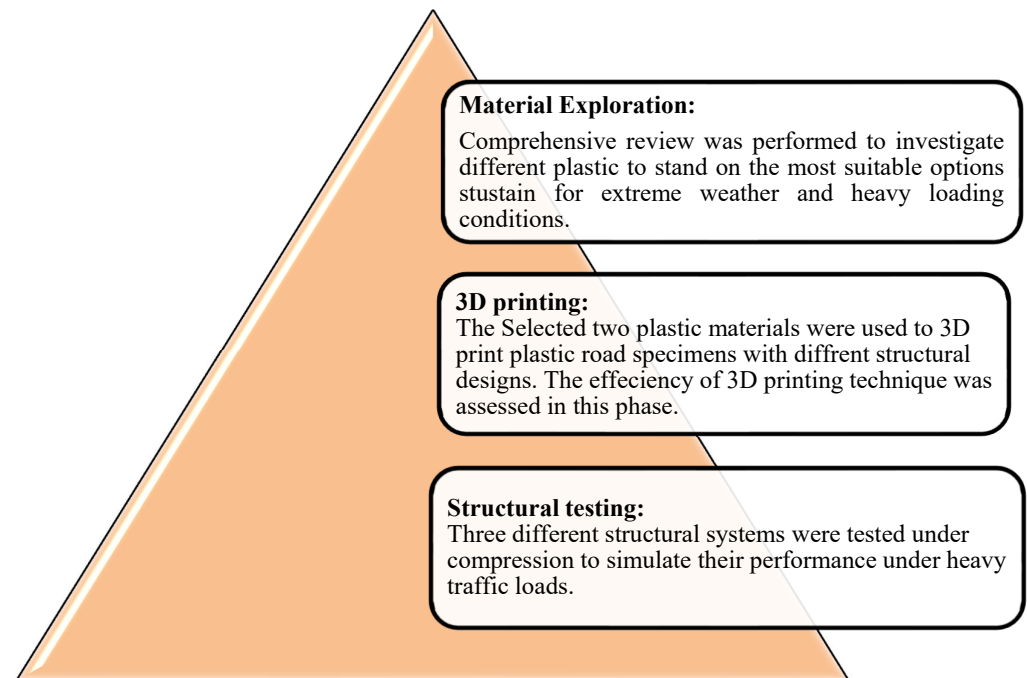


Figure 4. The three-phase methodology utilized in this study.

In the first phase, different materials were explored to determine the most suitable material for the hot weather and heavy loading conditions. An extensive review was performed to explore the chemical composition, engineering properties, characteristics, thermal stability, mechanical strength, and environmental impact of six different plastic materials. The considered plastic materials in this review were polylactic acid (PLA), acrylonitrile butadiene styrene (ABS), glycol-modified PET (PETG), thermoplastic polyurethane (TPU), polyamide (Nylon), and polycarbonate (PC). These six materials were selected as they are the most common plastic materials utilized as filaments for 3D printing.

Based on the outcomes of the first phase, the second phase was concerned with printing small-scale plastic road modules using the selected materials. In this phase, three different structural systems were designed using the Fusion 360 software (v2023). Then, the models were prepared in 3D printing stereolithography (STL) format. As shown in Figure 5, the first structural system consisted of modules with plastic columns, the second system consisted of modular units with solid plastic cones, and the third system consisted of modular units with X-bracing. The details of the three models' geometries, and details of each system's components, are explained in Figure 5. The S5 Ultimaker 3D Printer [16] was utilized in this experiment. The Ultimaker S5 3D Printer can print parts with a maximum size of $330 \times 240 \times 300$ mm. The 3D printer was set up and calibrated for optimal module printing performance. The time needed to print each model, the quality of the printed model, and the amount of plastic material used in the printing were assessed at the end of this phase.

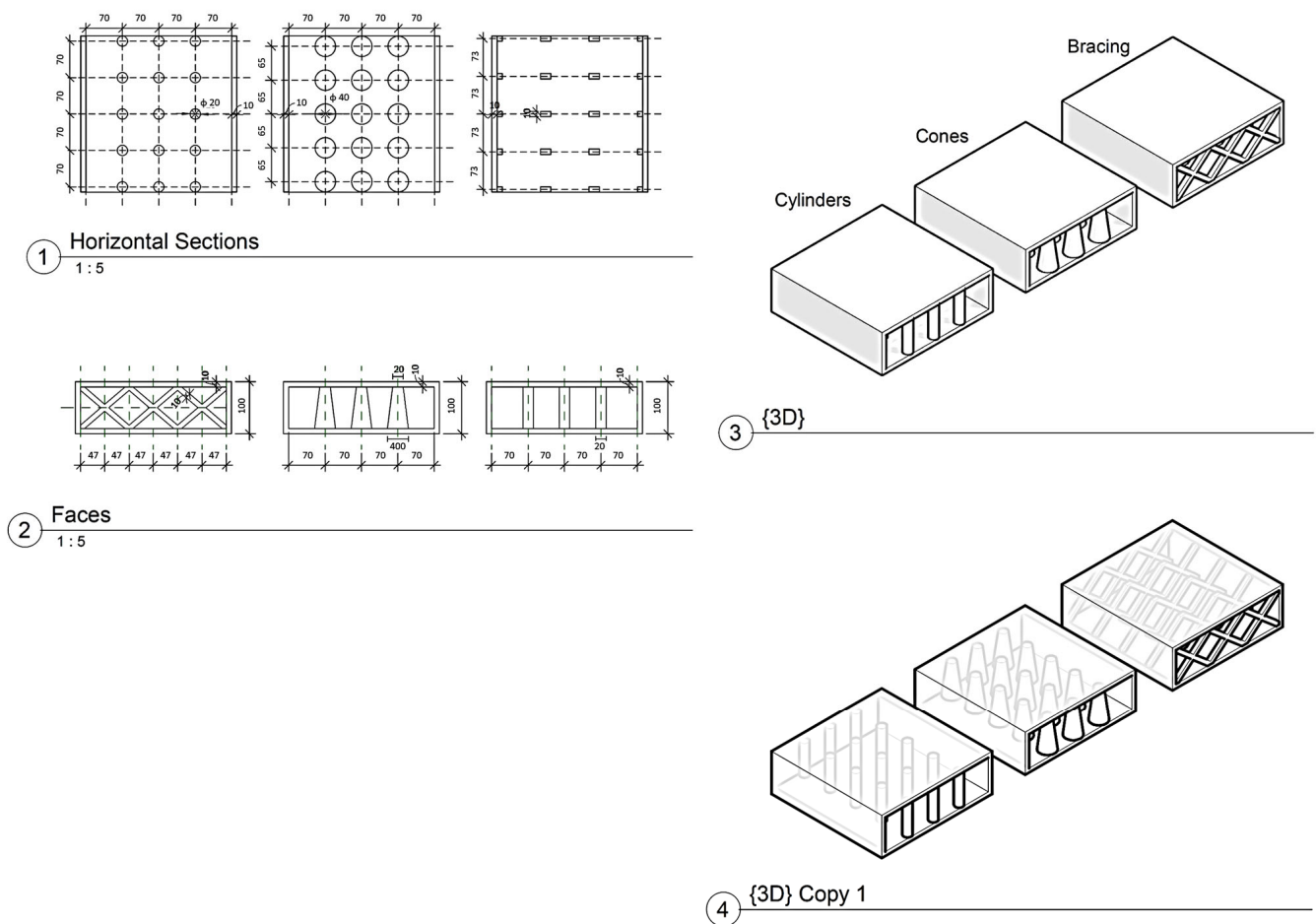


Figure 5. Details of the three structural models developed for 3D printing.

In the third phase, the three different structural systems (Figure 5), namely hollow modular with plastic columns, hollow modular with solid plastic cones, and hollow modular with X-bracing, were tested under compression [17] to investigate their structural performance under heavy traffic loads. A universal testing machine (UTM) was used for the compression tests. This machine is capable of the low-force, low-torque testing of mechanical parts down to 0.0005 N [18]. The data collected from the tests were analyzed and evaluated to draw conclusions about the feasibility of using 3D printing technology for the manufacturing of plastic road modules and the potential benefits of different structural systems.

4. Potential Plastic Materials for Advanced Applications

Plastic materials have gained a significant place in the manufacturing industry owing to their versatility and wide range of properties. The use of plastic in road construction has also attracted attention in recent years due to its potential to provide a sustainable solution for road construction. With the advent of 3D printing technology, plastic materials can now be used to create prefabricated modular road sections, which can offer numerous advantages over traditional road construction techniques.

The current modular plastic panels are made from a combination of virgin and recycled plastic materials [14]. The utilization of plastic waste as a raw material in the prefabrication of plastic pavements constitutes a global innovation ecosystem in recycling plastic waste. The utilized plastic material has several advantages, such as high melting point temperatures, typically beyond 66 °C, and a smaller carbon footprint. Moreover, plastic pavements exhibit fewer defects, such as cracks or potholes, compared to conventional pavement types. However, as mentioned earlier, the current application of this system is

limited to light-traffic pavement. Special attention should be given to the material selection to extend this promising technology to fit heavier-traffic roadway applications.

This section explores the potential plastic materials suitable for advanced applications such as 3D-printed plastic roads. An extensive review of the properties and characteristics of different plastic materials, including their thermal stability, mechanical strength, and environmental impact, is conducted to identify the optimal material for use in this experimental study.

4.1. Polylactic Acid (PLA)

Polylactic acid (PLA) is a thermoplastic polyester that is biodegradable and compostable and is made from renewable resources such as maize starch, tapioca root, or sugarcane. PLA's popularity has grown in recent years as a result of its environmental friendliness and biodegradability. Due to its simplicity of use and compatibility with the majority of fused deposition modeling (FDM) printers, PLA is a widely used material in 3D printing. It is a relatively rigid material with good dimensional accuracy and stability, making it suitable for the creation of precise and intricate 3D models. It also has a low shrinkage rate, which reduces the risk of warping during printing [19].

The chemical structure of polylactic acid (PLA) is $(C_3H_4O_2)_n$, as shown in Figure 6a. PLA is created by either the ring-opening polymerization of lactide, a cyclic dimer of lactic acid, or by condensing lactic acid molecules with the loss of water. Depending on how the chiral carbon atoms are arranged, lactic acid can exist in two different enantiomeric forms: L-lactic acid and D-lactic acid. PLA can also have different stereochemical structures depending on the arrangement and ratio of the polymer chain's L- and D-lactic acid units. PLA's physical and mechanical characteristics, including its crystallinity, melting point, glass transition temperature, and tensile strength, are influenced by its chemical structure [20].

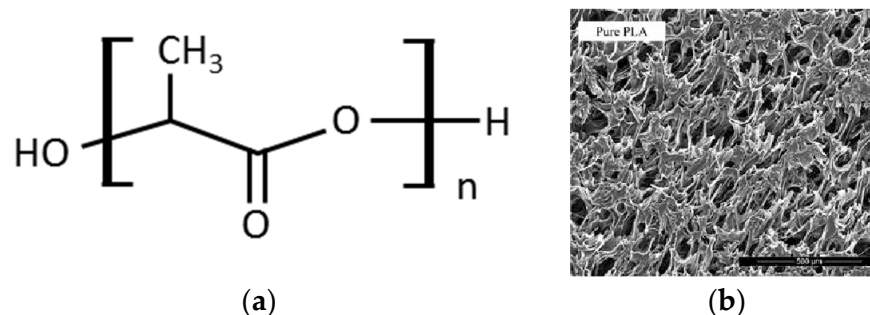


Figure 6. (a) Chemical structure of polylactic acid (PLA) $[(C_3H_4O_2)_n]$. (b) SEM micrographs for PLA (Pai, et al., 2020 [21]).

The microstructure of PLA materials (Figure 6b) depends on various factors, such as blending, processing, and compatibilization [22]. For example, when blended with another polymer, PLA can form different microstructures, such as sea island, interpenetrating networks, or co-continuous phases. Figure 6b shows the microstructure of the pure PLA material. A summary of the advantages, disadvantages, and engineering properties of the PLA material is given in Table 3.

4.2. Acrylonitrile Butadiene Styrene (ABS)

Acrylonitrile butadiene styrene (ABS) is a thermoplastic polymer characterized as a heterogeneous multi-phase system. ABS is created by polymerizing styrene and acrylonitrile with polybutadiene. It has a glass transition temperature of about 105 °C [23]. ABS plastic is known for its toughness, impact resistance, and lightness, as well as its easy machinability, moldability, and fabricability. It is stable up to its melting point and may be heated, cooled, and reheated multiple times without degrading [24]. ABS plastic is also used in diverse industries and applications, such as automotive parts, electronic

housing, musical instruments, and 3D printing. Furthermore, some studies have used ABS to improve the performance of modified asphalt binders, making them suitable candidates for use in plastic pavement applications (e.g., [25]).

Acrylonitrile, butadiene, and styrene are the three monomers that form ABS plastic's chemical structure. The chemical formula for acrylonitrile butadiene styrene ($C_8H_8C_4H_6C_3H_3N$) is shown in Figure 7a [26]. The ratios might range from 5% to 30% butadiene, 40% to 60% styrene, and 15% to 35% acrylonitrile. On the other hand, the microstructure of ABS is composed of a long polybutadiene chain interspersed with shorter poly(styrene-co-acrylonitrile). Because they are polar, the nitrile groups from nearby chains attract one another and bind together, making ABS more robust than pure polystyrene, as shown in Figure 7b.

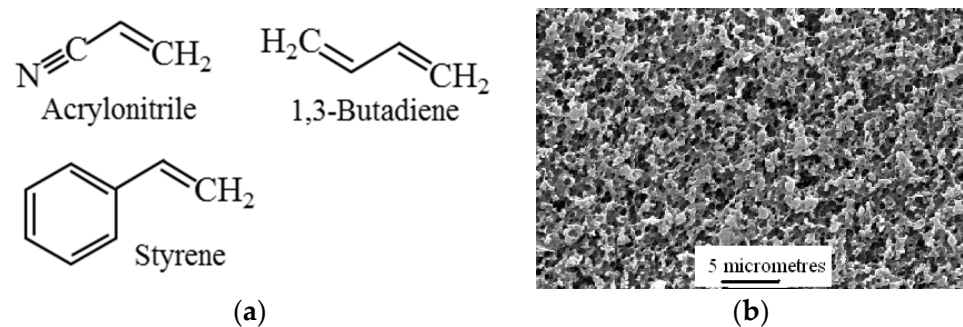


Figure 7. (a) Acrylonitrile butadiene styrene (ABS) chemical structure. (b) SEM micrographs for ABS (after Dechaisit and Trakarnpruk, 2011 [27]).

4.3. Polyethylene Terephthalate Glycol (PETG)

Polyethylene terephthalate glycol is a thermoplastic material that is frequently used in 3D printing because of its superior mechanical properties, durability, and simplicity of usage. It is a modified version of polyethylene terephthalate (PET), which is widely used for packaging applications, but with added glycol to improve its flexibility and impact resistance. PETG has high transparency and is resistant to impact, chemicals, and weathering, making it an ideal material for high-strength and -durability applications. It is also easy to print with, as it has a low shrinkage rate, making it less likely to warp or crack during printing. PETG is commonly used in medical equipment, food packaging, and outdoor signs due to its high resistance to UV light and weathering. It is also extensively used in 3D printing since the glycol minimizes the difficulties involved with PET, including overheating, high humidity, and frailty. PETG products can also be sanitized. PETG is emerging as the ideal type for 3D printing due to the strong adhesion between sheets, minimal distortion during printing, resilience in low-temperature environments, chemical endurance towards bases and acids, and lack of aroma when printing [28].

When cyclohexane dimethanol is added to the polymer chain, PET can be copolymerized to form polyethylene terephthalate glycol-modified (PETG). Hence, the chemical composition of PETG is $(C_{10}H_8O_4)_x \cdot (C_{10}H_{14}O_4)_y \cdot (C_2H_6O_2)_z$, where x , y , and z are the respective mole fractions of terephthalic acid, cyclohexanedimethanol, and ethylene glycol used in the production process [29]. The resulting polymer has a flexible and amorphous structure due to the inclusion of cyclohexanedimethanol, which provides flexibility to the material, making it more impact-resistant compared to other polyester materials like PET, as shown in Figure 8.

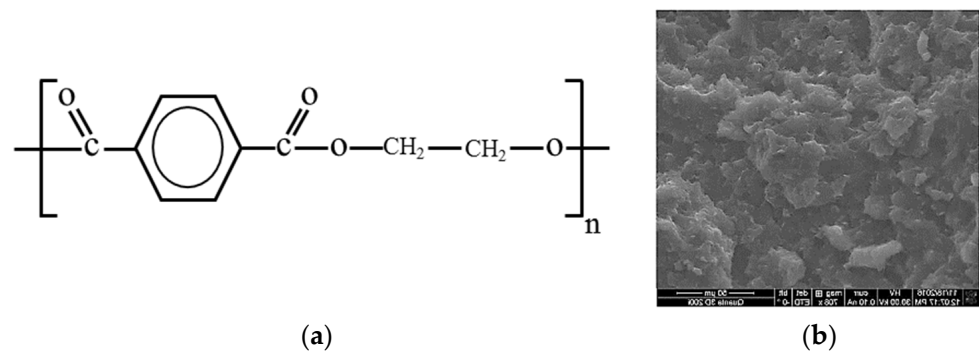


Figure 8. (a) PETG's chemical structure. (b) SEM micrographs for PETG (after [30]).

4.4. Thermoplastic Polyurethane (TPU)

Thermoplastic polyurethane, often known as TPU, is a form of polyurethane plastic that possesses a variety of features, such as elasticity, transparency, and resistance to abrasion, oil, and grease. In scientific terms, it is classified as a thermoplastic elastomer and is composed of linear segmented block copolymers that include both flexible and stiff segments [31]. The production of TPU is accomplished through the reaction of diisocyanates with short-chain diols (also known as chain extenders) and long-chain diols. It is possible to construct a large range of TPUs, each with its own unique set of characteristics, by adjusting the reaction chemicals' proportions, structures, and molecular weights. Figure 9 shows the typical chemical formation and the microscope structure of the TPU.

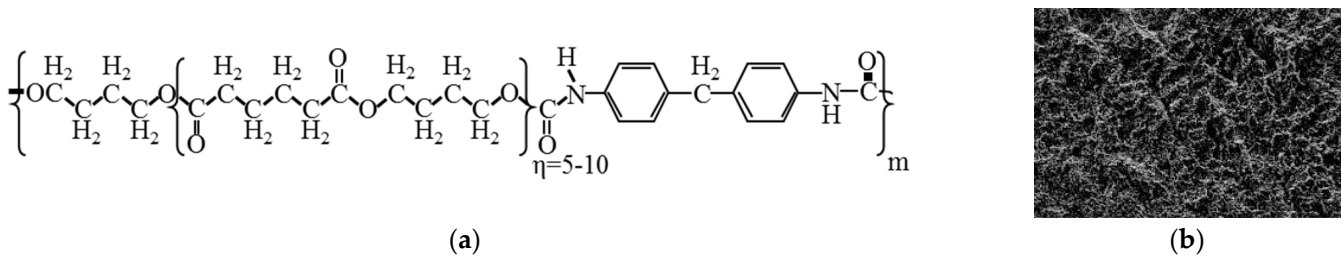


Figure 9. (a) Molecular structure of thermoplastic polyurethanes [32]. (b) SEM micrographs for TPU (after [33]).

4.5. Polyamide (Nylon)

Polyamide, also known by its brand name "Nylon", is a type of man-made plastic material that is formed of polyamides with a high molecular weight. It is most commonly produced as a fiber, although it can also be made into molded items and other shapes. Polyamides can be produced either through the polycondensation of a dicarboxylic acid with a diamine or through the self-condensation of an amino acid that possesses the ability to polymerize. It is feasible to manufacture items that are either stiff and brittle or soft and rubbery by adjusting the acid and the amine proportions in the recipe [34,35].

One of the numerous attributes of Nylon is a high level of resilience to wear, as well as heat and chemicals. When cold-drawn, it possesses robustness, elasticity, and toughness. Nylon is used in a wide variety of applications, including automotive instrument panels, caster wheels, power tools, sporting goods, medical devices, drive belts, footwear, inflatable rafts, fire hoses, and a variety of extruded film, sheet, and profile uses. Some of these applications are more common than others. The microstructure of polyamides, particularly those produced from primary amines, is characterized by a high degree of crystallinity. This is especially the case for polyamides derived from primary amines. When the specimen is subjected to tension, the orientation of the molecules continues until the length of the specimen is approximately four times its initial value. Figure 10 shows the typical chemical formation and the microscope structure of Nylon 66.

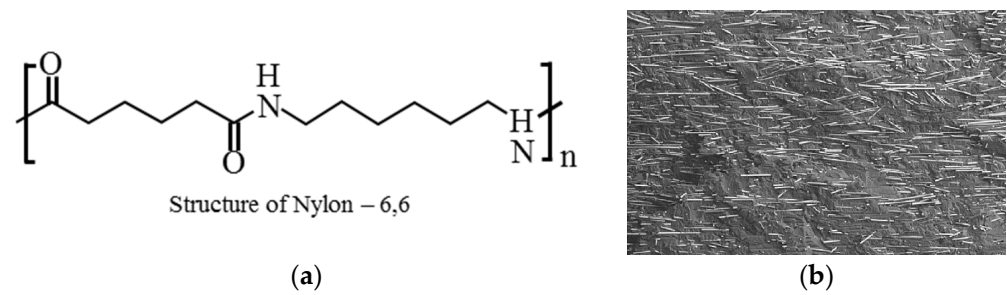


Figure 10. (a) Microstructure of the Nylon material. (b) SEM micrographs for Nylon (after [34,35]).

4.6. Polycarbonate

Polycarbonate (PC) is a type of thermoplastic polymer that is known for its strength, transparency, and resistance to impact. It is composed of repeating units of bisphenol A and phosgene, which are chemically linked together to create a strong and durable material [36]. Polycarbonate (PC) material is suitable for 3D printing. It is a popular choice for 3D printing because of its high strength, heat resistance, and impact resistance. However, it may require a higher printing temperature and slower printing speed compared to other materials. It is also important to ensure that the 3D printer used is capable of printing with PC. Figure 11 shows the typical chemical formation of the PC material.

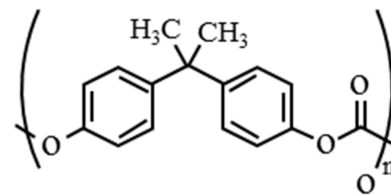


Figure 11. The chemical composition of PC material.

Table 3. A summary of the advantages, disadvantages, and engineering properties of six plastic materials for 3D printing applications.

| No. | Flament Type | Material | Advantages | Disadvantages | Typical Mechanical Properties | | | | | Reference |
|-----|--------------|---------------------------------|--|---|---------------------------------|---|----------------------|---------------------|---------------------------|------------|
| | | | | | Glass Transition Temperature °C | Melting Temperature °C | Tensile Strength MPa | Young's Modulus GPa | Density g/cm ³ | |
| 1 | PLA | Polylactic Acid | <ul style="list-style-type: none"> It is environmentally friendly and can be composted under industrial conditions. It is easy to print with and does not require a heated bed or an enclosed chamber. It has good dimensional accuracy and surface quality. It has a wide range of colors and blends available. It has good biocompatibility, biodegradability, and optical clarity. | <ul style="list-style-type: none"> It is brittle and prone to cracking under stress or impact. It has poor thermal stability and can deform or degrade at high temperatures or under UV light. It has low resistance to chemicals and solvents. It has poor adhesion to some materials and may require a special coating or glue. One potential drawback of PLA is its sensitivity to high temperatures, which can cause the deformation or melting of the material. PLA has lower impact resistance and toughness compared to other 3D printing materials like ABS or Nylon. | 60 | 170 | 50 MPa | 2.7 to 3.0 GPa | 1.25 g/cm ³ | [19,37–39] |
| 2 | ABS | Acrylonitrile Butadiene Styrene | <ul style="list-style-type: none"> Durable, heat-resistant, and impact-resistant. High rigidity, good weldability, and insulating properties. Good resilience to impact, even in wintry weather. Good abrasion and strain resistance. Strong mechanical stability with time. Bright surfaces with great aspect ratios. | <ul style="list-style-type: none"> Prone to warping, emits fumes when printing. Weatherability (damaged by sunlight). Solvent resistance. Hazardous when burned. Higher price than polystyrene or polyethylene. | 105 | ABS is amorphous and therefore has no true melting point. | 43 | 2.28 | 1.03 to 1.06 | [40,41] |

Table 3. Cont.

| No. | Flament Type | Material | Advantages | Disadvantages | Typical Mechanical Properties | | | | | Reference |
|-----|--------------|-----------------------------------|--|--|---------------------------------|------------------------|----------------------|---------------------|---------------------------|------------|
| | | | | | Glass Transition Temperature °C | Melting Temperature °C | Tensile Strength MPa | Young's Modulus GPa | Density g/cm ³ | |
| 3 | PETG | Polyethylene Terephthalate Glycol | PETG is suited for high-strength display units, attributable to its rigidity and impact resistance. It is also ideal for 3D printing. PETG is a vacuum and thermoformable polymer that can resist high pressures without disintegrating. It may be molded or extruded into sheets in a number of different ways. PETG is inherently translucent, allowing for distinctive effects, but it can also be readily colored and combined to provide a variety of forms. While 3D printing, PETG is non-toxic and odorless. | It is more prone to leaking than PLA or ABS, and it would require extra post-processing to erase any flaws. If not stored in a dry environment, it will absorb water, making components fragile. If the PETG filament is not properly disposed of, it might have a harmful influence on the environment. The PETG filament does not have high cosmetic print quality. It is also sensitive to the print speed and requires a higher process temperature to finish. | 81 °C. | 260 °C | 270 MPa | 2.1 | 1.23 | [42,43] |
| 4 | TPU | Thermoplastic Polyurethane | Thermoplastic polyurethane (TPU) is a flexible filament often used in FDM 3D printing to create parts that require flexibility, strength, and durability. Some advantages of using TPU for 3D printing include its high durability, flexibility, and excellent tensile strength. It has a greater glass transition temperature than PLA and can handle low temperatures well without becoming brittle. TPU is also chemically and abrasion-resistant, making it suitable for functional flexible prototype testing. | There are also some challenges associated with 3D printing with TPU. It is generally regarded as a difficult material to print with due to its softness, which can make it more difficult to consistently extrude the appropriate amount of filament. | −40 °C to 55 °C | 185–243 °C | 28.0–96.0 MPa | 0.621–5.50 GPa | 1.28–1.66 | [32,44,45] |

Table 3. Cont.

| No. | Flament Type | Material | Advantages | Disadvantages | Typical Mechanical Properties | | | | | Reference |
|-----|--------------|---------------|--|--|---------------------------------|------------------------|----------------------|---------------------|---------------------------|-----------|
| | | | | | Glass Transition Temperature °C | Melting Temperature °C | Tensile Strength MPa | Young's Modulus GPa | Density g/cm ³ | |
| 5 | Nylon 66 | Polyamide | <ol style="list-style-type: none"> 1. Durable: Nylon fibers are tough and resistant to wear and tear, making it a popular material for clothes and outdoor equipment. 2. Lightweight: Nylon is a lightweight material, which makes it easy to carry and use in various applications. 3. Resistant to moisture: Nylon is moisture-resistant, preventing water from being absorbed and keeping the material dry. 4. Affordable: Nylon is an affordable material compared to other synthetic and natural fibers. 5. Versatile: Nylon can be molded into various shapes and sizes, making it appropriate for a wide range of products and applications. | <ol style="list-style-type: none"> 1. Prone to melting: Nylon will melt if exposed to high heat, which can be a disadvantage in certain applications. 2. Low breathability: Nylon is not breathable like natural fibers, which can cause comfort issues when used in clothing. 3. Static electricity: Nylon fibers can generate static electricity, causing discomfort and annoyance for some users. 4. Environmental impacts: Nylon is a synthetic fiber made from petrochemicals, meaning that it is not biodegradable and has a significant environmental impact. | 47 | 258 | 85 | 3.50 GPa | 1.15 | [34,46] |
| 6 | PC | Polycarbonate | <ol style="list-style-type: none"> 1. High impact resistance: PC material is known for its exceptional impact resistance, making it an ideal choice for products that require durability. 2. Lightweight: Compared to other materials, such as metal, PC material is relatively lightweight, making it an excellent choice for products that need to be easy to handle and transport. 3. Transparency: PC material is transparent, which makes it an ideal choice for products that require clarity. 4. Resistance to high temperatures: PC material is resistant to high temperatures, which makes it an excellent choice for products that need to withstand heat. | <ol style="list-style-type: none"> 1. Scratches: Despite its strength and durability, PC material is prone to scratches, which can impact its appearance and functionality. 2. Chemical sensitivity: PC material can be sensitive to certain chemicals, which can cause it to degrade over time. 3. Cost: PC material can be more expensive than some other materials, such as acrylic, which may impact its use in certain products. 4. UV sensitivity: PC material can be sensitive to UV rays, which can cause it to yellow over time. | 141–150 °C | 250–343 °C | 65.5 Mpa | 2.38 GPa | 1.03 | [36,47] |

5. Experimental Setup and Testing

The 3D printing technology was chosen for the manufacturing of the plastic road modules due to its potential to provide the structural design flexibility required for the design of different plastic models that could be customized for various purposes, such as sustaining heavy traffic loads or withstanding extreme weather conditions. Accordingly, the S5 Ultimaker 3D Printer [16] was set up and calibrated for optimal module printing performance. Then, it was used to print the three different structural systems. Figure 12a shows the printing processes for one of the 3D models. In general, the three models required almost the same time of 18 h to be printed. Figure 12b shows the printed models of the three structural systems. The three models were printed with the same size of $150 \times 150 \times 50$ mm and a thickness of 5 mm.

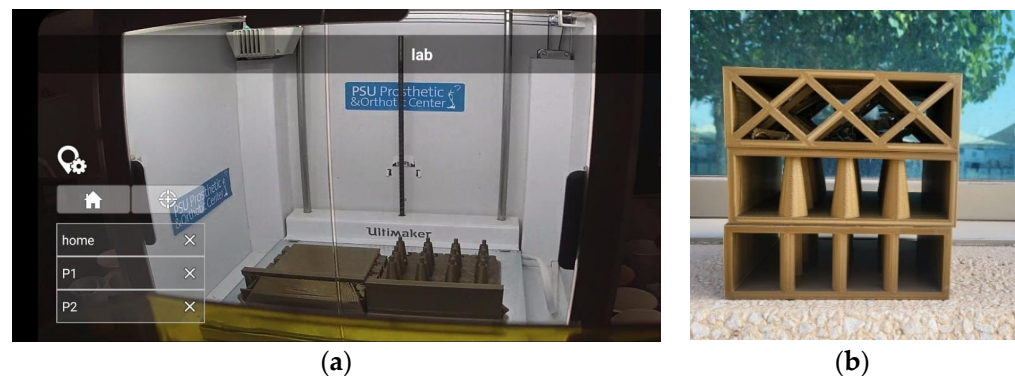


Figure 12. (a) A snapshot of the 3D model printing process. (b) Three models for the proposed three structural systems of the plastic roads.

After careful consideration of the properties and characteristics of the six potential plastic materials reviewed in the previous section, and based on the availability of the plastic filament, the study selected PLA and PETG for further investigation. PLA was chosen due to its environmental sustainability, biodegradability, and ease of use in 3D printing. It is a renewable resource, making it an ideal choice for sustainable and eco-friendly applications. Moreover, its rigidity and high modulus of elasticity make it an excellent choice for the creation of structural elements. In addition, it has low toxicity, making it safe to handle and dispose of. PETG, on the other hand, was the second selected material due to its superior thermal resistance, durability, and resistance to impact and UV radiation. These properties make it an ideal material for heavy traffic applications and extreme weather conditions. It is commonly used in automotive and medical applications, where durability and toughness are critical. Both PLA and PETG are widely available and compatible with most 3D printers, making them suitable for the study's experimental design. Table 4 summarizes the main characteristics of the two materials.

Table 4. Comparison between the principal characteristics of PLA and PETG.

| Property | PLA | PETG |
|------------------------|-------------------------------------|---|
| Strength | Brittle, low impact resistance | Tough, high impact resistance |
| Flexibility | Rigid, minimal flexibility | Flexible, high elongation at break |
| Durability | Biodegradable, degraded in UV light | Non-biodegradable, resists UV degradation |
| Printability | Easy to print, low warping | More difficult to print, higher warping |
| Temperature Resistance | Melts at around 60–65 °C | Melts at around 80–85 °C |
| Chemical Resistance | Sensitive to chemicals | Resistant to chemicals |

Three PLA models were printed and tested for their performance under heavy traffic loads through a series of compression load tests (ASTM D695 [17]) performed on each system, to evaluate their structural performance and determine the optimal design, as shown in Figure 13. Data collected from the three tests were analyzed and evaluated to draw conclusions about the feasibility of using 3D printing technology for the manufacturing of plastic road modules and the potential benefits of using the PLA material. Then, the same process was repeated but using the PETG material, as shown in Figure 13d.

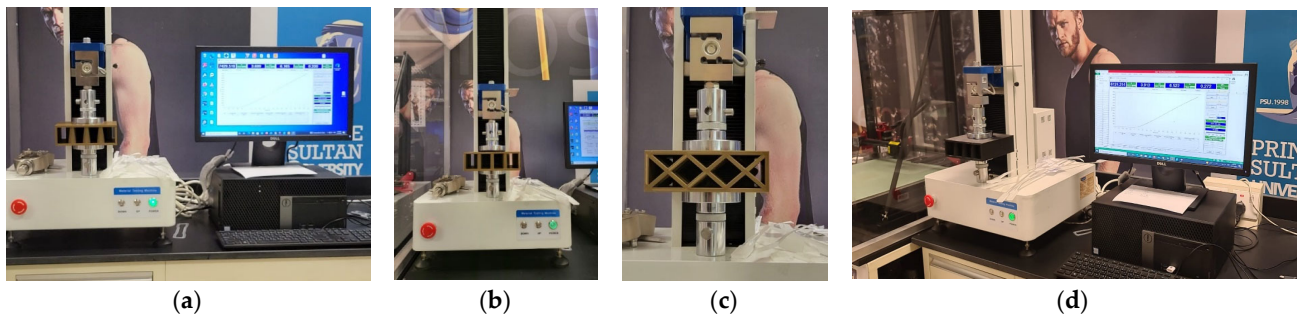


Figure 13. The compression tests performed to examine the structural performance of the three proposed systems of 3D printed plastic roads, as small models made of PLA material. (a) Hollow modular with solid plastic cones. (b) Hollow modular with plastic columns. (c) Hollow modular with X-bracing. (d) A sample of the 3D-printed plastic PETG model.

6. Results and Discussion

The study aspired to investigate the feasibility of utilizing the 3D printing technique to provide the thermal and structural flexibility required to develop 3D-printed plastic models for road segments able to withstand heavy traffic and extreme weather conditions. The success of 3D-printed plastic roads requires careful consideration of the plastic materials used. This study reviewed six plastic materials for their suitability in 3D-printed plastic roads: PLA, ABS, PETG, TPU, Nylon, and PC. The review evaluated their thermal stability, mechanical strength, and environmental impact. After careful consideration, PLA and PETG were selected as the most suitable plastic materials for 3D-printed plastic roads. This section discusses the results of the performed experimental tests to examine the reliability of the 3D printing technique in providing the structural design flexibility required to develop advanced plastic roads.

6.1. Structural Design Flexibility

The structural performance of three hollow modular systems made of PLA material was examined in compression based on the ASTM D695 [17] standard. The systems were modular with columns, modular with cones, and modular with X-bracing. The obtained stress–strain relationships of the three systems are given in Figure 14.

The stress–strain relationship of each of the three systems provides insights into their structural performance under compression. The modular system with cones was able to sustain stress up to 0.435 MPa without reaching failure, indicating its ability to withstand higher loads. This system also had a relatively high strain of 9.4, indicating its flexibility under compression. Similarly, the modular system with columns was also able to sustain stress up to 0.435 MPa with a strain of 8.9. These results demonstrate the structural design flexibility provided by 3D printing technology, as both systems were able to withstand heavy loads while maintaining their structural integrity. Nevertheless, the modular system with X-bracing exhibited failure at a stress level of only 0.25 MPa, suggesting that the strength of the bracing design was insufficient to endure heavy loads. Further optimization may be necessary to enhance its structural stability.

The results of the compression tests conducted on the three modular systems made of PLA material indicated the potential of using 3D printing to produce printed plastic pavement modules with various structural capacities and stiffnesses. The modular systems

with cones and columns exhibited promising results in terms of their ability to withstand heavy loads and maintain their structural integrity, while the X-bracing system showed a high degree of flexibility and failed in a ductile way.

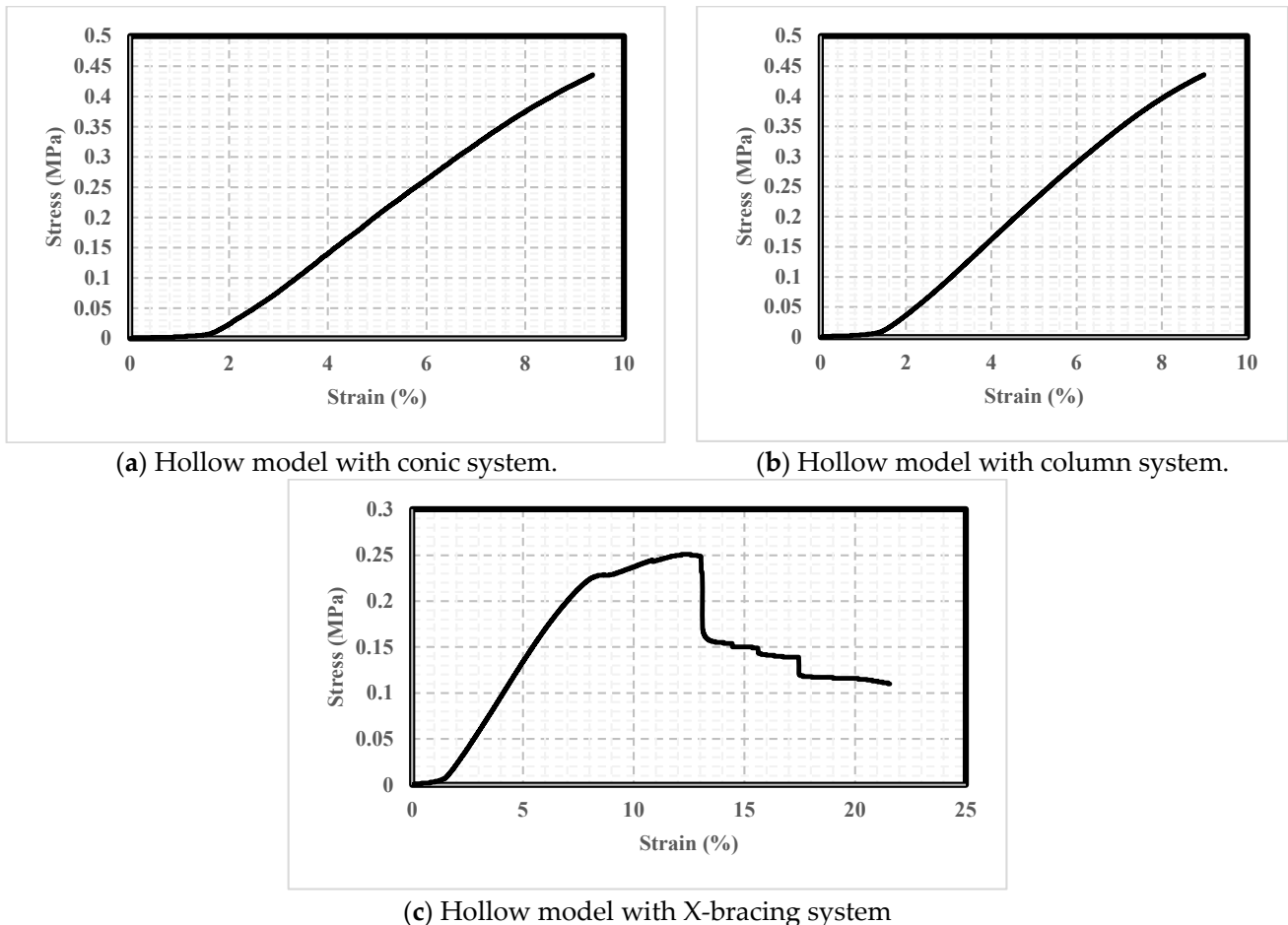


Figure 14. Stress–strain relationships of the three PLA hollow models.

6.2. Deformability and Failure Mode

The load–displacement results obtained for the three PLA models with different structural systems are presented in Figure 15. It can be observed that the modular system with cones exhibited the highest compression strength, as it was able to sustain a maximum load of 9.3 kN without failure, with maximum deformation of 4.84 mm. The modular system with columns also demonstrated relatively good performance, with almost the same maximum load of 9.3 kN but with higher maximum deformation of 5.393 mm. In contrast, the modular system with X-bracing showed lower compression strength, achieving failure under a load of 5.4 kN, and failed in a ductile manner with maximum displacement of 12.5 mm.

Furthermore, Figure 16 presents the deformed shape of the model that achieved failure (X-bracing system) and the second that only deformed without achieving failure (column system). It can be observed that the model with X-bracing exhibited significant plastic deformation before failing, indicating that this system is not suitable for heavy traffic applications. The cone and column systems, on the other hand, showed relatively smaller deformation before reaching their maximum load-carrying capacities, indicating their potential for use in structural applications where high load-carrying capacities and minimal deformation are required. The following section explores the performance of this system upon using different plastic materials (PETG), to investigate its performance in extreme weather conditions.

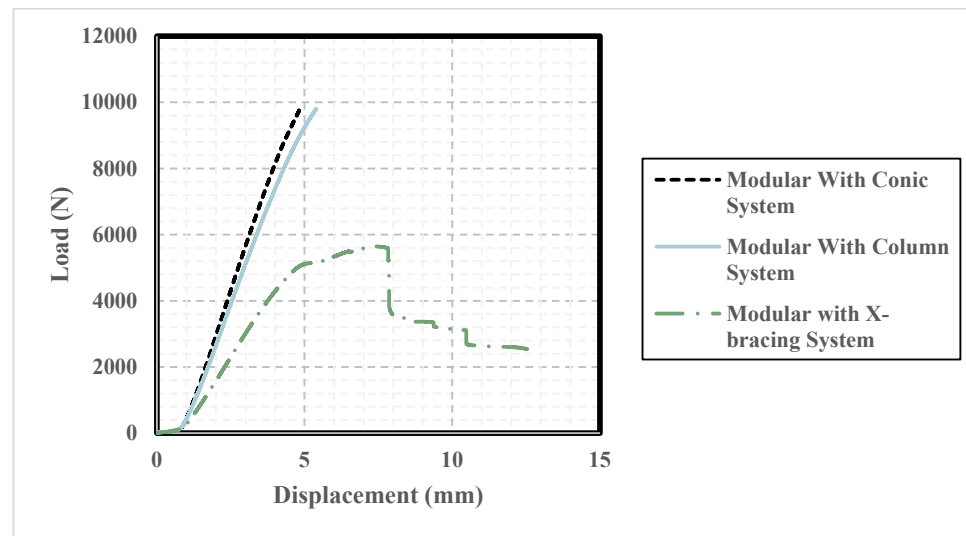


Figure 15. A comparison between the load–displacement relationships of the three PLA models with different structural systems.

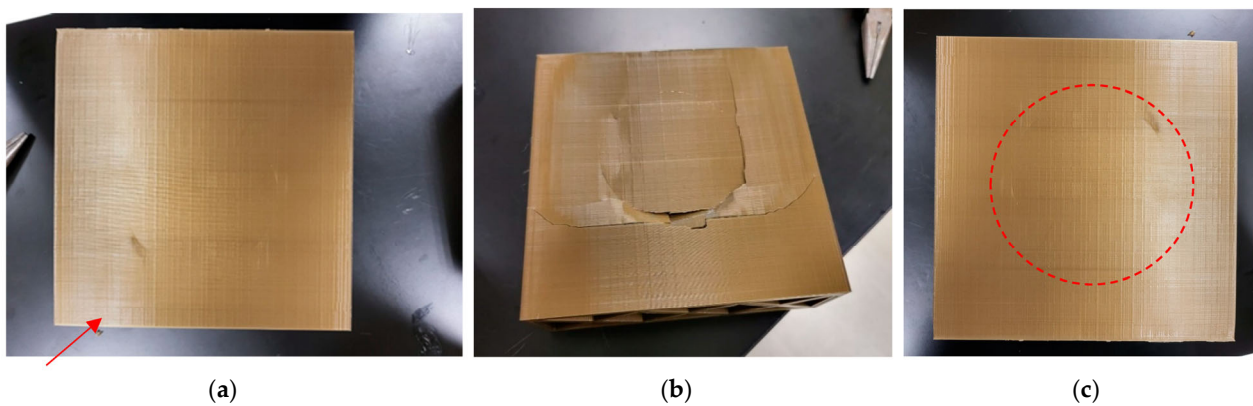


Figure 16. The deformed shape of two different PLA models with different structural systems. (a) Hollow model with column system, (b) Hollow model with X-bracing system, (c) Hollow model with cone system.

6.3. PLA vs. PETG: Comparative Analysis

The heat deflection temperature (HDT) test was performed by Roman et al., 2021 [48] for two plastic materials (PLA and PETG) at 0.45 Mpa according to ISO 75 [49], to measure the amount of heat that a plastic can withstand before it matures under a specified load. In addition, the maximum melting temperature for the same two materials was obtained according to ISO 11357, while the glass transition temperature and modulus of elasticity were determined using the ASTM E1356 and ASTM D638 [50], respectively. Table 5 summarizes the determined properties of both PLA and PETG.

Based on the comparative analysis provided, it is evident that PETG exhibits superior thermal stability when compared to PLA. Specifically, PETG demonstrates several advantages in key thermal properties. First, PETG displays a notably higher heat deflection temperature (HDT) at 0.45 MPa, registering at 68 °C, which surpasses the HDT of PLA, recorded at 55 °C, as per the ISO 75 test. Moreover, PETG exhibits an impressive maximum melting temperature range of 220–245 °C, significantly higher than PLA's range of 145–160 °C, as determined by the ISO 11357 test. Furthermore, PETG displays a superior glass transition temperature, ranging from 80 to 82 °C, in contrast to PLA's range of 55–60 °C, as established through the ASTM E1356 test. This robust comparison clearly highlights PETG as the more thermally stable material in contrast to PLA.

Table 5. Thermal properties of PLA and PETG (after Roman et al., 2021 [48]).

| Test | Unit | Typical Properties | | | |
|---|------|--------------------|----------------|---------|-----------------|
| | | PLA | Reference | PETG | Reference |
| Heat deflection temperature (HDT) at 0.45 Mpa | °C | 55 | ISO 75 [49] | 68 | ISO 75 [49] |
| Elasticity modulus | GPa | 2.3 | ASTM D638 [50] | 2.1 | ASTM D638 [50] |
| Maximum melting temperature | °C | 145–160 | ISO 11357 [51] | 220–245 | ISO 11357 [51] |
| Glass transition temperature | °C | 55–60 | ISO 11357 [51] | 80–82 | ASTM E1356 [52] |
| Elongation at flow | % | 2% | ASTM D638 [50] | 14% | ASTM D638 [50] |
| Final traction force | MPa | 26.4 | ASTM D638 [50] | 45.8 | ASTM D638 [50] |

It is also interesting to mention that, compared to Bitumen 62, which is commonly utilized in asphalt production, PLA has a heat deflection temperature of 55 °C and a melting temperature of 152 °C, while PETG has a heat deflection temperature of 68 °C and a melting temperature of almost 232 °C. Meanwhile, Bitumen 62 has a melting temperature range of 100–150 °C and a heat deflection temperature of around 60 °C. With this in mind, PETG could have superior thermal stability even compared to Bitumen.

On the other hand, the compression test was conducted on the hollow modular system made of PETG material with a conic structural system. The stress–strain relationship of the PETG model is shown in Figure 17a, and the deformed shape of the model is presented in Figure 17b.

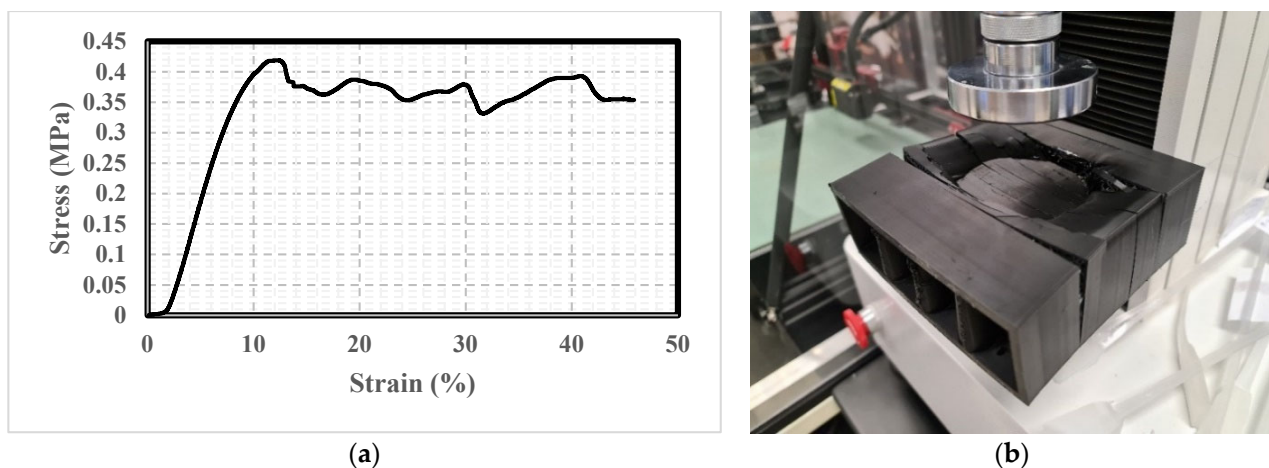


Figure 17. (a) Load–displacement relationship of a PETG model with a conic structural system. (b) The deformed shape of a PETG model with a conic structural system.

The results show that the PETG model exhibited relatively ductile behavior under compression. As shown, the conic structural system made of PETG material demonstrated compression strength comparable to that of the PLA model, achieving failure at a stress of 0.419 MPa, but with a significant strain of 45. Figure 18 compares the load–displacement relationships of the conic models with PLA and PETG materials.

The mechanical behavior of the PETG and PLA models was investigated through compression tests, and the results demonstrated significant differences in their responses to the applied loads. The PETG model showed relatively ductile behavior, achieving failure at a maximum load of 9.3 kN and a large displacement of 27.52 mm. In contrast, the PLA model demonstrated more brittle behavior, failing at a lower load of 9.5 kN with a maximum displacement of 9.4 mm. The load–displacement relationships of the two conic models further emphasize these differences, highlighting the unique mechanical properties of each material. With this in mind, as shown in Table 5, the PETG material has superior thermal properties, as it has higher melting, heat deflection, and glass transition

temperatures compared to PLA. These thermal properties may have contributed to the observed differences in mechanical behavior between the two materials.

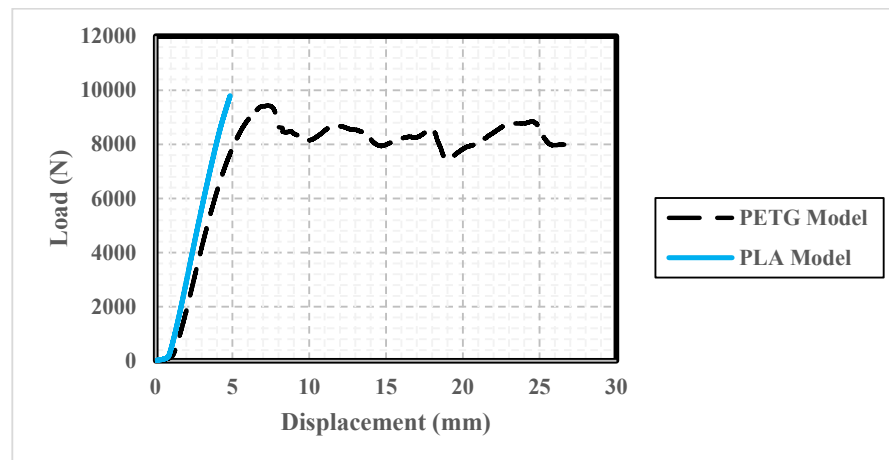


Figure 18. A comparison between load–displacement relationships of the two conic models with PLA and PETG materials.

6.4. Hybrid Material and Nano-Additives

The use of hybrid plastic materials in 3D printing offers several advantages over using a single material. Hybrid materials can combine the desirable properties of two or more materials, creating parts with unique properties tailored to specific applications. For example, a hybrid material could combine the strength and stiffness of one material with the flexibility and durability of another, resulting in a part that is both strong and resilient.

The results of the comparative analysis highlighted that the modular system with cones made of PLA material exhibited the highest compression strength, sustaining the maximum stress without failure. On the other hand, the system made of PETG material, although using the same conic structural system, demonstrated relatively ductile behavior with a significant displacement before failure; nevertheless, PETG had superior thermal stability. Therefore, to achieve optimal performance that fits the structural and thermal requirements, the study suggests a hybrid system combining the two materials, which may result in a system with improved overall performance, as the PETG material could be used for the modular body to provide flexibility and ductility, while the PLA material could be used for the cones to provide strength and rigidity.

Nano-additives could also offer added value as materials that are added to a base material at the nanoscale to improve its properties. In the case of 3D printing, nano-additives can be added to the hybrid material to improve its mechanical, electrical, or thermal properties, as well as to enhance its biocompatibility or other characteristics. Examples of nano-additives that can be used in hybrid materials for 3D printing include graphene, carbon nanotubes, metallic nanoparticles, and ceramic nanoparticles. These nano-additives can be incorporated into the hybrid material through processes such as dispersion, blending, or coating.

7. Conclusions

This preliminary study aimed to explore the viability of employing 3D printing technology for the production of plastic pavement modules, presenting an alternative to the conventional use of asphalt in road construction. Conventional asphalt production and construction are associated with substantial carbon emissions, which are contributing factors to global warming and climate change. To address this critical issue, this study proposes an innovative solution involving 3D-printed prefabricated plastic panels as an eco-friendly and sustainable substitute for traditional road pavements.

The PlasticRoad technology has shown great promise in addressing these challenges in different infrastructure projects. According to the review presented in this study, implementing the PlasticRoad technology in ten case studies demonstrated its versatility and ability to store and filter rainwater to prevent flooding and mitigate drought. However, the current application was limited to sidewalks and light-load cycling lanes due to the prefabrication limitation. In contrast to the methods described in CCL100 to 300, which primarily focus on prefabricated approaches and recycled plastics, this study explored the innovative realm of 3D printing technology, employing two distinct types of plastic filament, namely polylactic acid (PLA) and polyethylene terephthalate glycol (PETG). Therefore, the feasibility of 3D printing technology was examined in providing the required design flexibility to produce hollow modular plastic pavement systems that can sustain heavy traffic and extreme weather conditions.

Initially, six plastic materials were reviewed, and polylactic acid (PLA) and polyethylene terephthalate glycol (PETG) were identified as the most suitable materials for the 3D printing of the pavement modules. Then, three different structural systems were designed and printed using the two adopted materials and a 3D printer: hollow modular with plastic columns, hollow modular with solid plastic cones, and hollow modular with X-bracing.

The study included compression tests on the three structural systems to assess their performance under heavy traffic loads. The findings pointed to the superiority of the conic structural system for hollow modular systems. Specifically, the PLA cones displayed the highest compression strength, whereas the PETG system exhibited relatively ductile characteristics and superior thermal stability. The study recommends the utilization of a hybrid system comprising PLA and PETG materials to enhance the overall performance by integrating flexibility and strength, potentially enhancing the resistance to extreme weather and heavy traffic conditions.

The study concludes that 3D printing technology has the potential to revolutionize the road construction industry by providing more sustainable solutions for infrastructure development. By replacing conventional asphalt with 3D-printed plastic pavement modules, the carbon emissions associated with the production and construction of asphalt can be reduced, contributing to climate change mitigation. Further research is recommended to explore the durability and long-term performance of 3D-printed plastic pavement modules under different environmental conditions and traffic loads.

8. Limitations and Future Studies

This study has several limitations that need to be acknowledged. Firstly, this preliminary study focused solely on the feasibility of using 3D printing technology to provide the required structural design flexibility for the manufacturing of plastic pavement modules that can sustain heavy traffic and extreme weather conditions. Therefore, further studies are needed to investigate the long-term performance of the developed systems in actual road conditions. Secondly, only six types of plastic materials were evaluated for 3D printing, and only two of them (PLA and PETG) were identified as the most suitable materials for this study. Other materials with better performance may exist, and future studies should investigate a broader range of materials for the 3D printing of plastic roads. In addition, only three types of hollow modular systems were designed and tested, and other structural designs should be explored to optimize the performance of 3D-printed plastic roads. Finally, while the use of recycled plastics in the production of plastic roads can reduce CO₂ emissions, the environmental impact of producing and disposing of 3D printing filaments should be considered in future studies.

Examining the performance of the large-scale 3D-printed plastic road models under different cyclic and thermal loads will be essential to validate the performance of this class of roads under heavy loads and extreme weather conditions.

The development of 3D-printed plastic roads has opened the door to the integration of various smart technologies for future city applications. The use of sensors embedded in the pavement can provide real-time data on traffic flow, allowing for dynamic routing

and optimizing travel times. The incorporation of solar cells in the pavement can enable energy harvesting, reducing the reliance on external power sources and contributing to the sustainability of the road network. Furthermore, these intelligent plastic roads can also be equipped with communication technologies, allowing for vehicle-to-infrastructure (V2I) and vehicle-to-vehicle (V2V) communication, which is essential for the efficient operation of autonomous vehicles. Ultimately, the integration of these smart technologies into 3D-printed plastic roads can enhance the safety, efficiency, and sustainability of the transportation network, contributing to the development of future cities.

Author Contributions: Conceptualization, M.E.A.-A. and J.A.; methodology, M.E.A.-A., D.A. and J.A.; software, Y.M.; validation, M.E.A.-A., J.A. and Y.M.; formal analysis, J.A.; investigation, D.A.; resources, D.A.; data curation, M.E.A.-A.; writing—original draft preparation, J.A., D.A. and Y.M.; writing—review and editing, M.E.A.-A.; visualization, D.A. and Y.M.; supervision, M.E.A.-A.; project administration, J.A.; funding acquisition, M.E.A.-A. All authors have read and agreed to the published version of the manuscript.

Funding: Prince Sultan University partly funded this research with grant number PSU-CE-SEED-2023. In addition, it was supported by the Structures and Material (S&M) Research Lab of Prince Sultan University.

Conflicts of Interest: The authors declare no conflict of interest.

References

- How Asphalt Is Contributing to Global Emissions—World Economic Forum. World Economic Forum. 2020. Available online: <https://www.weforum.org/agenda/2020/09/asphalt-bulding-carbon-emissions-global-warming/> (accessed on 26 March 2023).
- Mallick, R.B.; Chen, B.-L.; Bhowmick, S. Harvesting energy from asphalt pavements and reducing the heat island effect. *Int. J. Sustain. Eng.* **2009**, *2*, 214–228. [[CrossRef](#)]
- Al-Atroush, M.E. Structural behavior of the geothermo-electrical asphalt pavement: A critical review concerning climate change. *Heliyon* **2022**, *8*, e12107. [[CrossRef](#)] [[PubMed](#)]
- Ma, F.; Sha, A.; Lin, R.; Huang, Y.; Wang, C. Greenhouse Gas Emissions from Asphalt Pavement Construction: A Case Study in China. *Int. J. Environ. Res. Public Health* **2016**, *13*, 351. [[CrossRef](#)] [[PubMed](#)]
- Espinoza, M.; Campos, N.; Yang, R.; Ozer, H. Carbon Footprint Estimation in Road Construction: La Abundancia–Florenia Case Study. *Sustainability* **2019**, *11*, 2276. [[CrossRef](#)]
- Stocker, T.; Qin, D.; Plattner, G.K.; Tignor, M.; Allen, S.; Boschung, J.; Nauels, A.; Xia, Y.; Bex, V.; Midgley, P. (Eds.) *IPCC Climate Change, 2013; The Physical Science Basis*, Cambridge Univ. Press: Cambridge, UK, 2018; Available online: https://www.ipcc.ch/site/assets/uploads/2018/03/WG1AR5_SummaryVolume_FINAL.pdf (accessed on 14 January 2023).
- Repair Priorities, Transportation for America, Taxpayers for Common Sense, Washington, DC. Available online: <https://t4america.org/wp-content/uploads/2019/05/Repair-Priorities-2019.pdf> (accessed on 14 January 2023).
- Huang, Y.H. *Pavement Analysis and Design*; Prentice-Hall: Upper Saddle River, NJ, USA, 1993.
- Al-Atroush, M.E.; Bala, N.; Adamu, M. *Prefabricated Plastic Pavement for High-Traffic and Extreme Weather Conditions*; Hamdan, A., Aldhaen, E.S., Eds.; Artificial Intelligence and Transforming Digital Marketing. Studies in Systems, Decision and Control; Springer: Cham, Germany, 2024; Volume 487. [[CrossRef](#)]
- Al-Atroush, M.E.; Marouf, A.; Aloufi, M.; Marouf, M.; Sebaey, T.A.; Ibrahim, Y.E. Structural Performance Assessment of Geothermal Asphalt Pavements: A Comparative Experimental Study. *Sustainability* **2022**, *14*, 12855. [[CrossRef](#)]
- Gudipudi, P.P.; Underwood, B.S.; Zalghout, A. Impact of climate change on pavement structural performance in the United States. *Transp. Res. Part D Transp. Environ.* **2017**, *57*, 172–184. [[CrossRef](#)]
- Al-Qadami, E.H.H.; Mustafa, Z.; Al-Atroush, M.E. A numerical approach to understand the responses of passenger vehicles moving through floodwaters. *J. Flood Risk Manag.* **2022**, *15*, e12828. [[CrossRef](#)]
- Wavin. 6 January 2021. The World’s First Plastic Road Opens in The Netherlands. Wavin. Available online: <https://blog.wavin.com/en-gb/plastic-road-launch> (accessed on 26 March 2023).
- PlasticRoad. Available online: <https://plasticroad.com/> (accessed on 14 January 2023).
- Kamal, I.; Bas, Y. Materials and technologies in road pavements an overview. *Mater. Today Proc.* **2021**, *42*, 2660–2667. [[CrossRef](#)]
- Ultimaker. The S5 Ultimaker 3D Printer. Available online: <https://ultimaker.com/> (accessed on 26 March 2023).
- ASTM D695-15; Standard Test Method for Compressive Properties of Rigid Plastics. American Society for Testing and Materials. ASTM International: West Conshohocken, PA, USA, 2015. [[CrossRef](#)]
- Jinan Hensgrand Instrument Co., Ltd. (n.d.). Electronic UTM. Available online: <https://www.utmchina.net/> (accessed on 1 August 2023).
- Harpool, T.D.; Alarifi, I.M.; Alshammari, B.A.; Aabid, A.; Baig, M.; Malik, R.A.; Sayed, A.M.; Asmatulu, R.; El-Bagory, T.M.A.A. Evaluation of the Infill Design on the Tensile Response of 3D Printed Polylactic Acid Polymer. *Materials* **2021**, *14*, 2195. [[CrossRef](#)]

20. Södergård, A.; Stolt, M. Industrial Production of High Molecular Weight Poly (Lactic Acid). In *Poly (Lactic Acid): Synthesis, Structures, Properties, Processing, and Applications*; Auras, R., Lim, L.T., Selke, S.E., Tsuji, H., Eds.; John Wiley & Sons: Hoboken, NJ, USA, 2010; pp. 27–41. [CrossRef]
21. Pai, F.-C.; Chu, H.-H.; Lai, S.-M. Preparation and properties of thermally conductive PLA/PA 610 biomass composites. *J. Elastomers Plast.* **2020**, *52*, 53–69. [CrossRef]
22. Zhao, X.; Li, J.; Yu, X.; Yang, S.; Liu, J.; Zhou, W.; Peng, S. Microstructure and barrier properties of reactive compatibilized PLA/PA11 blends investigated by positron annihilation lifetime spectroscopy. *Polym. Test.* **2022**, *115*, 107763. [CrossRef]
23. Rahman, M.; Schott, N.R.; Sadhu, L.K. Glass Transition of ABS in 3D Printing. In Proceedings of the 2016 COMSOL Conference in Boston, Boston, MA, USA, 12 October 2016.
24. Edward, N.P. *Plastics: Thermoplastics, Thermosets, and Elastomers, Handbook of Materials Selection*; John Wiley & Sons, Inc.: New York, NY, USA, 2002; pp. 363–365. ISBN 978-0-471-35924-1.
25. Hasan, M.R.M.; Colbert, B.; You, Z.; Jamshidi, A.; Heiden, P.A.; Hamzah, M.O. A simple treatment of electronic-waste plastics to produce asphalt binder additives with improved properties. *Constr. Build. Mater.* **2016**, *110*, 79–88. [CrossRef]
26. Turku, I.; Kasala, S.; Kärki, T. Characterization of Feedstock Filament Extruded from Secondary Sources of PS, ABS and PVC. *Recycling* **2018**, *3*, 57. [CrossRef]
27. Dehasit, P.; Trakarnpruk, W. Ni Electroless Plating of ABS Polymer by Palladium and Tin-free Process. *J. Met. Mater. Miner.* **2011**, *21*, 19–27.
28. What Is PETG? (Everything You Need to Know). TWI Global. Available online: <https://www.twi-global.com/technical-knowledge/faqs/what-is-petg> (accessed on 28 March 2023).
29. Lukianchuk, I.; Tulashvili, Y.; Podolyak, V.; Horbariuk, R.; Kovalchuk, V.; Bazyl, S. Didactic Principles of Education Students 3D-printing. *IJCSNS Int. J. Comput. Sci. Netw. Secur.* **2022**, *22*, 443–450. [CrossRef]
30. Kováčová, M.; Kozakovičová, J.; Procházka, M.; Janigová, I.; Vysopal, M.; Černičková, I.; Krajčovič, J.; Špitalský, Z. Novel Hybrid PETG Composites for 3D Printing. *Appl. Sci.* **2020**, *10*, 3062. [CrossRef]
31. Thermoplastic Polyurethane. American Chemical Council. Available online: <http://polyurethane.americanchemistry.com/Introduction-to-Polyurethanes/Applications/Thermoplastic-Polyurethane> (accessed on 30 March 2023).
32. Comprehensive Guide on Thermoplastic Polyurethanes (TPU). Omnexus. Available online: <https://omnexus.specialchem.com/selection-guide/thermoplastic-polyurethanes-tpu> (accessed on 30 March 2023).
33. Frick, A.; Borm, M.; Kaoud, N.; Kolodziej, J.; Neudeck, J. Microstructure and thermomechanical properties relationship of segmented thermoplastic polyurethane (TPU). *AIP Conf. Proc.* **2014**, *1593*, 520. [CrossRef]
34. Jagadeesan, N.; Selvaraj, A.; Nagaraja, S.; Abbas, M.; Saleel, C.A.; Aabid, A.; Baig, M. Response Surface Methodology Based Optimization of Test Parameter in Glass Fiber Reinforced Polyamide 66 for Dry Sliding, Tribological Performance. *Materials* **2022**, *15*, 6520. [CrossRef]
35. Miled, B. *Coupled Viscoelastic-Viscoplastic Modeling of Homogeneous and Reinforced Thermoplastic Polymers*; Université Catholique de Louvain, Ecole Polytechnique de Louvain, Institute of Mechanics, Materials and Civil Engineering: Louvain, Belgium, 2011.
36. Li, Z.-M.; Qian, Z.-Q.; Yang, M.-B.; Yang, W.; Xie, B.-H.; Huang, R. Anisotropic microstructure-impact fracture behavior relationship of polycarbonate/polyethylene blends injection-molded at different temperatures. *Polymer* **2005**, *46*, 10466–10477. [CrossRef]
37. Liu, W.; Chen, P.; Wang, X.; Wang, F.; Wu, Y. Effects of Poly(butyleneadipate-co-terephthalate) as a Macromolecular Nucleating Agent on the Crystallization and Foaming Behavior of Biodegradable Poly(lactic acid). *Cell. Polym.* **2017**, *36*, 75–96. [CrossRef]
38. Nagarajan, V.; Mohanty, A.K.; Misra, M. Perspective on Polylactic Acid (PLA) based Sustainable Materials for Durable Applications: Focus on Toughness and Heat Resistance. *ACS Sustain. Chem. Eng.* **2016**, *4*, 2899–2916. [CrossRef]
39. Couture, A.; Lebrun, G.; Laperrière, L. Mechanical properties of polylactic acid (PLA) composites reinforced with unidirectional flax and flax-paper layers. *Compos. Struct.* **2016**, *154*, 286–295. [CrossRef]
40. What Is ABS Material? Plastic Extrusion Technologies. 8 October 2021. Available online: <https://plasticextrusiontech.net/what-is-abs-material/> (accessed on 30 March 2023).
41. Rogers, T. Everything You Need to Know About ABS Plastic. Creative Mechanisms, 13 July 2015. Available online: <https://www.creativemechanisms.com/blog/everything-you-need-to-know-about-abs-plastic> (accessed on 30 March 2023).
42. Simplify3D Software.(22 November 2022). Properties Table. Simplify3D Software. Available online: <https://www.simplify3d.com/resources/materials-guide/properties-table/> (accessed on 30 March 2023).
43. Kattan, M.; Dargent, E.; Ledru, J.; Grenet, J. Strain-induced crystallization in uniaxially drawn PETG plates. *J. Appl. Polym. Sci.* **2001**, *81*, 3405–3412. [CrossRef]
44. TPU. Treatstock. Available online: <https://www.treatstock.com/material/tpu> (accessed on 30 March 2023).
45. Overview of Materials for Thermoplastic Polyurethane, Elastomer, Glass Filled, Matweb (a) (n.d.). Available online: <https://matweb.com/search/datasheet.aspx?matguid=2fe782a31c4b4bed984b49651762b086&ckck=1> (accessed on 1 April 2023).
46. Baig, U.; Waheed, A.; Aljundi, I.H.; AbuMousa, R.A. Facile Fabrication of Graphitic Carbon Nitride Nanosheets and its Integrated Polyamide Hyper-Cross-linked TFC Nanofiltration Membrane with Intrinsic Molecular Porosity for Salts and Organic Pollutant Rejection from Water. *J. Mater. Res. Technol.* **2021**, *15*, 6319–6328. [CrossRef]
47. Overview of Materials for Polycarbonate, Extruded, Matweb (b) (n.d.). Available online: <https://www.matweb.com/search/DataSheet.aspx?MatGUID=501acbb63cbc4f748faa7490884cdbca&ckck=1> (accessed on 1 April 2023).

48. Roman, N.; Cojocaru, D.; Coman, C.; Repanovici, A.; Bou, S.F.; Miclaus, R.S. Materials for respiratory masks in the context of covid 19 pandemic. *Mater. Plast.* **2021**, *57*, 236–247. [[CrossRef](#)]
49. *ISO 75-1:2020*; Plastics—Determination of Temperature of Deflection under Load—Part 1: General Test Method. International Standards Organization: Geneva, Switzerland, 2013. Available online: <https://www.iso.org/standard/77576.html> (accessed on 24 February 2023).
50. *ASTM D638-14*; Standard Test Method for Tensile Properties of Plastics. American Society for Testing and Materials. ASTM International: West Conshohocken, PA, USA, 2014. [[CrossRef](#)]
51. *ISO E. 11357-1*; Plastics-Differential Scanning Calorimetry (DSC)—Part 1: General Principles, German Version. DIN Deutsches Institut Für Normung e: Berlin, Germany, 2017. Available online: <https://www.iso.org/standard/70024.html> (accessed on 24 February 2023).
52. *ASTM E1356-08*; Standard Test Method for Assignment of the Glass Transition Temperatures by Differential Scanning Calorimetry. American Society for Testing and Materials: West Conshohocken, PA, USA, 2008. [[CrossRef](#)]

Disclaimer/Publisher’s Note: The statements, opinions and data contained in all publications are solely those of the individual author(s) and contributor(s) and not of MDPI and/or the editor(s). MDPI and/or the editor(s) disclaim responsibility for any injury to people or property resulting from any ideas, methods, instructions or products referred to in the content.